이학석사 학위논문

Mechanism of KAI1 that regulated cell cycle in hematopoietic stem cell

조혈모세포의 세포주기를 조절하는 KAI1 유전자의 분자기전 연구

2015년 2월

서울대학교 대학원

분자 의학 및 바이오제약학과

이 환

Abstract

Hematopoiesis is regulated by quiescent long term repopulating hematopoietic stem cells (LT-HSCs) in the bone marrow (BM) niche. KAI1 belongs to tetraspanin superfamily and is known as suppressor of tumor metastasis. In this study, KAI1 was expressed selectively in LT-HSCs located in the BM, but not in other stem-progenitor cells. We generated $KAI1^{-/-}$ mice and observed that LT-HSCs selectively decreased in number because LT-HSCs lost quiescence. KAI1 repressed cell cycle by induction of TGF-β1/Smad3 signaling via PKC, leading to induction of CDK inhibitors and cycle arrest. After ablation of BM by 5-fluorouracil treatment, recovery of cells in the BM was significantly retarded in $KAI1^{-/-}$ mice. Mice that received $KAI1^{-/-}$ HSCs showed a decrease in LT-HSCs compared with those receiving WT-HSCs. KAI1 was expressed also in human LT-HSCs, and the majority of $KAI1^{+}$ LT-HSCs were quiescent. Thus, KAI1 is a previously unidentified functional surface marker of LT-HSCs and maintains LT-HSC quiescence.

KEYWORDS: LT-HSC, Quiescence, KAI1(CD82), Tetraspanin, Bone marrow, Stem cell niche

Student Number: 2013-22735

CONTENTS

List of Figures

Introduction

Hematopoietic stem cell transplantation is the most widely used regenerative therapy for a variety of life-threatening hematologic diseases. An essential factor for successful transplantation is fine adjustments in hematopoiesis as determined by hematopoietic stem cells (HSCs) residing in a specialized microenvironment, termed bone marrow (BM) niches (Calvi et al., 2003; Morrison and Scadden, 2014; Walkley et al., 2007). While most HSCs remain dormant during steady-state in the BM stem cell niche, they undergo cycles of quiescence and self-renewal depending on blood cell requirements, which are controlled by cell cycle regulators (Brenet et al., 2013b; Tesio and Trumpp, 2011; Zon,2008). In the hierarchical study of hematopoietic stem-progenitor cells (HSPCs), long term repopulating-hematopoietic stem cells (LT-HSCs) have the capability of selfrenewal that maintains lifelong production of all blood cell lineages, whereas multipotent progenitor cells (MPPs) provide only transient hematopoietic lineages (Doulatov et al.,2012). Although several

sets of cell surface markers that discriminate HSCs from other progenitors, such as MPPs, have been reported (Doulatov et al., 2012), the functional significance of these surface molecules remains elusive.

In addition to signature molecules in LT-HSCs, other important factors that may influence the behavior of HSCs, particularly quiescence versus proliferation, include various environmental factors within the BM, such as angiopoietin-1, osteopontin, stromal derived factor-1, thrombopoietin and hypoxia inducible factor-1 alpha (HIF-1α) (Arai et al., 2004; Stier et al., 2005; Sugiyama et al., 2006; Takubo et al., 2010; Yoshihara et al., 2007). We recently reported that *KAI1* posesses a hypoxia responsive element in its promoter region and that its expression is turned on in ischemic tissues (Kim et al., 2010). *KAI1*, also known as *CD82*, is a member of the tetraspanin superfamily and has been initially identified in studies of T-cell activation (Liu and Zhang, 2006; Miranti, 2009). Tetraspanins are a large family of evolutionally-conserved cell surface molecules that contain four transmembrane domains and are expressed in abroad range of organisms, including fungi (but not yeast), *Caenorhabditis*

elegans, insects, zebrafish, and mammals (Levy and Shoham, 2005). In particular, KAI1 has attracted attention because lower expression has been shown to be associated with progression of solid tumors, such as prostate, gastric, colon, bladder and breast cancers, and because it suppresses metastasis of a wide spectrum of tumors (Miranti, 2009). KAI1 is ubiquitously expressed and evolutionally conserved (Liu and Zhang, 2006), suggesting that it plays a significant role in various functions of non-tumor cells as well.

Thus, we generated *KAI1* knockout mice and examined the role of KAI1 in the BM stem cell niche. We found that KAI1 is an important signature molecule that selectively defines dormant LT-HSCs and represses cell cycle progression 1 by activating the TGF-β1/Smad3 axis and cyclin-dependent kinase (CDK) inhibitors, leading to maintenance of quiescent LT-HSCs.

Materials and Methods

Bone marrow transplantation

C57BL/6 (CD45.2) donor mice and *KAI1*$^{-/-}$ (CD45.2) mice with Lin$^-$ BM cells (1x10^5) were transplanted by systemic injection into each lethally irradiated (7 Gy) CD45.1 recipient mouse. Lin$^-$ BM cells were sorted by magnetic activated cell sorting (MACS) as previously described (Hur et al., 2007). BM cells of recipient mice were collected 16 weeks after transplantation. For secondary transplantation, recipient mice (CD45.1) were sacrificed 16 weeks after the primary transplant. We sorted Lin$^-$ cells from each CD45.1 recipient's bone marrow, and 5x10^5 cells were transplanted by cardiac injection into lethally irradiated (7 Gy) recipient B6boyj (CD45.1) mice. For competitive BM transplantation, C57BL/6 (CD45.2) and *KAI1*$^{-/-}$ mice (CD45.2) with Lin$^-$ cells (5x10^5) were sorted separately using MACS. Sorted cells were mixed with whole BM mononuclear cells (1x10^6) from CD45.1 mice, and mixed cells

were transplanted into lethally irradiated CD45.1 mice. After 16 weeks, we harvested recipient mouse B6boyj (CD45.1) BM cells for FACS analysis. We measured the reconstitution capacity of CD45.2 cells against CD45.1 cells by FACS analysis.

Immunofluorescence studies

Immunocytochemistry was performed as previously described with minor modifications (Hur et al., 2013). For staining LT-HSCs, ST-HSCs and MPPs, after fixation with 2% PFA and blocking for 1 hour at room temperature, cells were incubated with a primary antibody for 12 hours at 4℃. The cells were then washed and incubated with a secondary antibody for 1 hour at room temperature. Whole or section of BM staining were performed as previously described with minor modifications (Hooper et al., 2009; Kunisaki et al., 2013; Nombela-Arrieta et al.,2013). The following antibodies were used for immunocytochemistry, whole BM and BM section staining: CD9 (H-110), CD37 (K-13), CD82 (C-16), and CD151 (H-80), all from Santa Cruz; CD3e (145-2c11), CD45R (RA3-6132), Ter-119 (TER-119), Ly6G (12B6-8C5), and

CD41 (eBioMwReg30), all from ebioscience; CD48 (HM48-1), CD150 (TC15 12F12.2), and Sca-1 (E13-1161.7), all from Biolegend; and CD31 (MEC13.3) from Bdscience and Ve-cadherin (BV9) from Abcam. Confocal images were acquired using Zeiss LSM-710 META confocal microscope and ZEN 2008 analysis software.

EML cell culture

EML cells were maintained in medium containing stem cell factor (SCF) as previously described (Arai et al., 2004). EML cells were grown in IMDM containing 20%FBS and SCF (200 ng/ml, PeproTech).

Lentiviral transduction

For KAI1 knock-down in EML cells, three shRNA constructs targeting different regions of the *KAI1* gene were used (Sigma-Aldrich, TRCN0000042409, TRCN0000042410, TRCN0000042411). Non-Targeting shRNA Control Lentiviral particle (Sigma-Aldrich, SHC016V) was used as the shRNA

negative control. Transduction was performed according to manufacturer's instructions. At 48 hours after transduction, EML cells were selected in EML growth medium containing puromycin (2 μg/ml). Transduced EML cells were analyzed for knock-down efficiency using qRT-PCR.

For KAI1 over-expression in EML cells, mouse *KAI1* cDNA was obtained from R&D (RDC0331) and cloned into pLenti 6.3/v5-Dest (Invitrogen) using the gateway system in accordance with the manufacturer's instructions. KAI1 pLenti 6.3/V5-Dest with ViraPower Packaging Mix (Invitrogen) was transfected into 293FT cells using polyethylenimine (PEI) according to the manufacturer's instructions. After 48 hours, viral supernatants were collected, filtered, and enriched by ultracentrifugation. Next, EML cells were transduced by an enriched KAI1-expressing lenti-virus with polybrene (10 μg/ml). At 48 hours after transduction, EML cells were selected in EML growth medium containing blasticidin S (5 μg/ml).

Myelosuppression models

WT and *KAI1*$^{-/-}$ mice were IP injected with 250 mg/kg 5-FU (Sigma). On days 2, 5, 10 and 20 after 5-FU injection, FACS analysis of BM cells was performed. C57Bl/6 and *KAI1*$^{-/-}$ mice were sub-lethally irradiated at 2.3 Gy in an irradiator and killed at days 0, 3, 7 and 14. Total BM cells were counted using a Countess® Automated Cell Counter (Invitrogen) and analyzed using FACS.

RNA sequencing analysis

RNA sequencing reads were aligned to the mouse genome build mm9 (NCBI37) (Pruitt et al., 2007) using TopHat 2.0.9 (Trapnell et al., 2009) and bowtie 0.12.9 (Langmead et al., 2009) with parameters --segment-length 21, which allowed 2 mismatches in a read. Expression levels for 23,170 RefSeq genes were measured by reads per kilobase per million mapped reads (RPKM) (Mortazavi et al., 2008). Differentially expressed genes between conditions were tested by Cuffdiff. Differentially expressed genes were defined as having more than 2-fold changes and an adjusted p-value less than 0.05. Hierarchical clustering of samples was performed by R

(www.R-project.org). Heat maps of gene expression were plotted by R package 'gplots'. To examine changes in genes specific to the KEGG pathway, R package 'pathview' was used (www.bioconductor.org). Gene set enrichment analysis (GSEA) was conducted to show statistically significant and concordant differences between samples (Subramanian et al., 2007). Gene lists related with a specific function annotation of GO (Gene Ontology) were obtained from the Mouse Genome Informatics (MGI) database (http://www.informatics.jax.org). The RNA-seq data have been deposited in the Gene Expression Omnibus (GEO) database (GSE56867).

Flow cytometry

Under sterile conditions, the femur and tibia were excised and all connective tissue attached to bones was removed. BM cells were harvested from the femur and tibia by flushing the BM cavity with PBS. BM cells were dispersed by passing through a 100 μm strainer. After suspended BM cells were obtained, cells were separated into mononuclear cells by Histopaque-1083 (Sigma-Aldrich), washed once at 1800 rpm at 4℃ and

suspended in FACS buffer. Flow cytometry was performed as previously described with slight modifications (Passegue and Wagers, 2006; Wang et al., 2011). Flow cytometry analysis and sorting (BD Canto II, LSR II and FACS Aria III) were performed using several antibodies specific for the following: CD45.2 (104), CD45.1 (A20), Sca-1 (D7), CD34 (RAM34) CD127 (SB/199), CD48 (HM48-1), CD3 (145- 2C11), CD4(RM4-5), CD8a(53-6.7), CD51 (RMV-7), NK1.1 (PK136), CD31 (MEC 13.3), CD45 (30-F11), CD11b (M1/70), TER-119 (TER-119), Ly-6G and Ly-6C (RB6- 8C5), lineage antibody-cocktail (M1/70 RA3-6B2, 145-2C11, TER-119, RB6-8C5), lineage cocktail 1 (SK7, 3G8, SJ25C1, L27, MφP9, NCAM16.2 and GA-R2), CD34 (8G12), CD38 (HIT2), Ki-67 (B56), CD244 (2B4), and CD229.1 (30C7), all from BD Pharmingen; CD117 (2B8), F4/80 (BM8), CD135 (A2F10), and CD45RA (H100) Anti- LAP (TW7-16B4), all from e-Bioscience; CD16/32 (93) and CD150 (TC15-12F12.2) from Biolegend; anti TGF-βR2, TGF-βR1 (Cl141231), and KAI1 (423524), all from R&D systems; and Hechest33342 from Invitrogen. Appropriate secondary antibodies were used in several experiments.

Preparation of human umbilical cord blood cell

Cord blood was collected as follows. After delivery, the cord was clamped and cord blood was collected in a closed system from the umbilical vein using a heparin coated syringe. Donators were informed with consent guidelines of the Institutional Review Board (IRB) of the Seoul National University Hospital (IRB number: H-1210- 032-430). After collection, mononuclear-cells were obtained by Histopaque1077 as previously described with slight modifications (Hur et al., 2004).

Long term culture initiating cells (LTC-IC) assay

LSK cells were collected using FACS sorting. Enriched hematopoietic stem cells were co-cultured with a murine stromal cell (OP9) layer and inactivated by irradiation (30 Gy) from a γ-irradiator before one day prior to experiments. LSK (5x103) cells were cultured with irradiated stromal cells for 4 weeks in MyeloCult medium (StemCell technology)

supplemented with hydrocortisone. Half-medium was changed weekly. To measure long term culture initiating cells, a semisolid methylcellulose medium containing cytokines was used for 10 days. After 10 days in culture, colonies on the methylcellulose were counted.

Protein and RNA analyses

Western blot analysis was performed to determine protein levels of each established cell line. Protein extraction and western blot analysis procedures were performed as previously described. For Western blot analysis, we used several antibodies as follows: KAI1 (Santa Cruz Biotechnology), TGF-β1 (Abcam), TGFβR2 (Abcam), p- Smad3 (Cell Signaling Technology), t-Smad3 (Cell Signaling Technology), p-Smad2 (Cell Signaling Technology), t-Smad2 (Cell Signaling Technology), p21 (Santa Cruz Biotechnology), p27 (Santa Cruz Biotechnology), p57 (Sigma-Aldrich), p-Rb (Cell Signaling Technology), t-Rb (Cell Signaling Technology) and β-actin (Santa Cruz Biotechnology). RNA was extracted from TRIZOL (Invitrogen) or RNeasy RNA isolation kit (Qiagen). Total RNA

was reverse transcribed in to cDNA with amfirivert cDNA synthesis premix (Gendepot). Information of primers for RT-PCR (Table S1).

Statistics methods

Continuous data are presented as mean ± SEM and were compared using the two-tailed Student t test or the Mann-Whitney rank sum test, as appropriate. To compare multiple samples, statistical significance was assessed using a one-way ANOVA, and adjustment for multiple comparisons was done by Tukey's t-test or Tamhane test, as appropriate. In all cases, multiple experiments were performed (number of experiments are shown in each figure) independently to verify the reproducibility. For animal models, no randomization or blinding was used. No mice were excluded unless a pathologic disease unrelated to the experiment was found. Also we excluded mice that died after BM ablation. We excluded 0 to 4 mice per treatment. For each experiment we used 3 to 6 mice for each experiment. Due to the lack for preceding research to base sample size we performed multiple independent experiments.

A 2-sided probability value $p<0.05$ was considered statistically significant. Statistical tests were performed using the statistical package SPSS version 18 (SPSS Inc, Chicago, IL).

Results

1. Mechanism by which KAI1 represses cell cycle progression and maintains LT HSC quiescence

To investigate the signaling mechanisms by which KAI1 maintains LT-HSC quiescence, we performed a series of *in vitro* gain- or loss-of-function experiments by gene transfection using an EML cell line considered an acceptable surrogate for studying HSPCs due to the difficulty in obtaining primary cells (Wu et al., 2012; Ye et al., 2005;Zou et al., 2011). For these experiments, we established stable EML cell lines by *KAI1* knock down using lentivirus-encoding shRNA (Figure S1A). Likewise, we generated a stable *KAI1* over expressing EML cell line using a lentivirus (Figure S3B). We confirmed the influence of KAI1 in the EML cell line because *KAI1* was expressed only in the Lin^- $CD34^-$ fraction, which is known to be quiescent at G0/G1 phase, but was not expressed in the Lin^- $CD34^+$ population, which is known to be active in the EML cell cycle (Zou et al.,2011) (Figure S2).

In RNA-sequencing (RNA-seq) analysis, we confirmed that CDK inhibitors, such as p21, p27 and p57, were down-regulated in KAI1 knock down EML cells by the shKAI1 lentivirus compared to KAI1 over-expressing EML cells (Figure 1A). Interestingly, RNAseq showed that TGFβ signal components as upstream of CDK inhibitor also change upon *KAI1* expression (Figure 1A and S3).

KAI1 knock down in EML cells decreased *TGF-β1* and *TGFβR2* expression at both the mRNA and protein levels, while *KAI1* overexpression increased expression, although *TGFβR1* was not affected (Figure 1B-1E). We confirmed reduction in *TGF-β1* and *TGFβR2* by *in vitro* knock down of KAI1 in EML cells in a separate experiment using LT-HSCs from the BM of $KAI1^{-/-}$ or WT mice. The frequency of LT-HSCs that were positive for TGF-β1 and TGFβR2 in FACS analysis was significantly lower in $KAI1^{-/-}$ than WT mice, but TGFβR1 was not affected by KAI1 in this experiment (Figure 1F and 1G). To investigate the functional link between KAI1 and TGF-β1, we evaluated PKC and Erk pathways that are known to be upstream regulators of TGF-β1 (Grewal et al., 1999; Shen et al., 2008). KAI1 significantly induced both expression and

secretion of TGF-β1, which were attenuated only by a PKC inhibitor, but not by an Erk inhibitor (Figure 1H and 1I). These data indicate that KAI1 augments gene expression and secretion of TGF-β1 through the PKC pathway.

Because CDK inhibitors, such as, p21, p27 and p57, were reported as downstream targets of the TGF-β/Smad3 pathway (Li et al., 1995), we examined the activation of Smad2/3, which is downstream of the TGF-β/TGF-β receptor (Sims-Robinson et al. 2012). KAI1 induced phosphorylation of Smad3 only, increased CDK inhibitors, and inhibited Rb phosphorylation, whereas the KAI1 knock down had opposite results (Figure 2A and 2B). Induction of CDK inhibitors by KAI1 was blocked by the TGF-β receptor inhibitor SB431542 and TGF-β1 neutralization (Figure 2C and 2D). KAI1 overexpression repressed cell cycle progression from the G0/G1 to S phase (Figure 2E) and increased the proportion of quiescent EML cells, such as the $Lin^{-}CD34^{-}$fraction rather than $Lin^{-}CD34^{+}$ population which is known to be active in cell cycling (Figure 2F). KAI1 represses the cell cycle and maintains quiescence of LT-HSCs through induction of the TGF-β1/Smad3 signaling via PKC, leading to induction of CDK inhibitors and cell cycle

arrest at transition from G0/G1 to S phase.

2. KAI1 in LT-HSCs and BM reconstitution after ablation

To examine the pivotal role of KAI1 in maintaining quiescent LT-HSCs and reconstituting the BM after ablative intervention, we monitored sequential changes in KAI1-positive LT-HSCs and proliferating blood cells in the BM after single dose treatment of 5-FU with sub-lethal irradiation in WT mice. Because 5-FU treatment induces apoptosis primarily inactively cycling progenitors or blood cells, the number of cells in the BM was rapidly decreased (Figure 3A), necessitating a new cell supply from quiescent LT-HSCs that survived 5-FU treatment. In response to the decreased number of cells in the BM, KAI1 expression in LT-HSCs started to decline on the 2nd day, reached nadir at the 5th day, and returned approximately 2 weeks after 5-FU treatment (Figure 3B and 3C). Reduction of KAI1 in LT-HSCs at the 5th day was accompanied by the start of cell proliferation in the BM (Figure 3D and 3E), indicating that KAI1 plays a pivotal role in maintaining quiescent LT-HSCs under normal conditions, but is suppressed to supply new

cells in response to BM ablation by releasing LT-HSCs from quiescence to proliferation and differentiation.

To obtain direct evidence that KAI1-positive LT-HSCs play an important role in hematopoietic recovery after BM ablation, we compared recovery of total or LSK cells in BM after sub-lethal irradiation between *KAI1*$^{-/-}$ mice and WT. Recovery of total or LSK cells in BM was significantly retarded in *KAI1*$^{-/-}$ mice compared to WT (Figure 3F and 3G).

3. KAI1 in LT-HSCs and long term reconstitution after BM transplantation

To investigate whether KAI1 affects the long term repopulating capacity of HSCs, we performed competitive BM transplantation (BMT) in which lethally irradiated recipient mice (CD45.1) were transplanted with HSPC-enriched 1x10^5 Lin(-) BM cells (CD45.2) from WT or *KAI1*$^{-/-}$ mice plus 5x10^5 competitor cells (CD45.1) (Figure 4A). At the 16th week after competitive BMT, we assessed chimerism of donor-derived cells (CD45.2) in the peripheral blood (PB) of recipient mice (CD45.1). Repopulating abilities of *KAI1*$^{-/-}$ cells were inferior

to those of WT cells (Figure 4B). In the serial BMT, the BM of mice that received HSPCs from *KAI1*$^{-/-}$ mice at the second BMT showed a decrease in LSK and LT-HSCs compared with those receiving HSPCs from WT mice (Figure 4C and 4D). We evaluated the cell cycle status in CD34^{-} LSK cells in recipients derived from donor *KAI1*$^{-/-}$ mice versus WT. The proportion and number of LT-HSCs (gated on CD34^{-} LSK cells) in G0 was significantly greater in recipients receiving HSPCs from WT mice than in those receiving HSPCs from *KAI1*$^{-/-}$ mice (Figure 4E). The direction of differentiation in LT-HSCs was different depending on the donor: HSCs from donor *KAI1*$^{-/-}$ showed preferential differentiation toward a myeloid lineage (Figure 4F). These tendencies were observed in fresh BM from WT and *KAI1*$^{-/-}$ mice (Figure S4A), which was corroborated by RNA-seq of EML cells in which *KAI1* knock down decreased gene expression of negative regulators for myeloid differentiation (Figure S4B). Collectively, these data indicate that KAI1 plays a significant role in maintaining the long term repopulating capacity of HSCs and that *KAI1* deficient HSCs show myeloid-biased differentiation.

There data showed that KAI1 plays a pivotal role in

maintaining quiescent LT-HSCs under normal conditions, but is suppressed to supply new cells in response to BM ablation by releasing LT-HSCs from quiescence to proliferation and differentiation.

4. Human KAI1-positive LT-HSCs from umbilical cord blood are quiescent

We examined human LT-HSCs from umbilical cord blood to confirm that KAI1 is a signature molecule that maintains LT-HSC quiescence, as observed in mice. We evaluated KAI1 expression in the human LT-HSC gate on $Lin^-CD38^-CD34^-CD93^+CD45RA^-$ (Anjos-Afonso et al., 2013) and identified two distinct populations. One quarter of human LT-HSCs were positive for KAI1 (Figure 4G), and most of the human KAI1-positive LT-HSCs stayed in the G0 phase, which differed from KAI1-negative cells (Figure 4H). These data indicate that KAI1 is expressed also in human LT-HSCs and that the majority of KAI1-positive LT-HSCs are quiescent.

Discussion

In this study, we provide evidence that KAI1 is not only a specific marker of dormant LT HSCs in the BM stem cell niche, but is also a key molecule in maintaining HSC quiescence. The underlying mechanism by which KAI1 maintains quiescence is activation of the TGF-α/SMAD signaling pathway and CDK inhibitors (p21, p27 and p57), which leads to cell cycle arrest at G0/G1 to S phase and subsequent quiescence of LT-HSCs in the BM niche (Figure 4I).

Mechanism by which KAI1 represses the cell cycle and maintains LT-HSC quiescence

A previous study reported that TGFβ-SMAD signaling is integral to BM recovery after ablation (Brenet et al., 2013a). In the present study, we demonstrated both uspstream and downstream mechanisms for TGFβ-SMAD signaling in regulating BM recovery. In RNA-seq and western blot analyses,

we showed that KAI1 turns on TGFβ signaling. With additional experiments using blockers, we confirmed that KAI1 increases the activity and amount of TGFβ through the PKC pathway and that the TGFβ-SMAD pathway stimulates CDK inhibitors, resulting in cell cycle arrest at the G1/S phase and LT-HSC quiescence. This pathway was confirmed using *KAI1* knockout mice and a *KAI1* knock down HSPC cell line in which TGFβ1 and phospho-SMAD3 protein expression was reduced.

Previous studies have reported that CDK inhibitors, such as p21, p27 and p57, are known to be associated with quiescence and self-renewal (Cheng et al., 2000; Matsumoto et al., 2011; Tesio and Trumpp, 2011; Zou et al., 2011). A recent study reported that p57 and p27 actively participate in maintaining HSC quiescence and that p27 compensates for loss of function caused by down regulation of p57 in maintaining HSC quiescence (Zou et al., 2011). In the present study, we revealed the upstream mechanism of CDK inhibitors in regulating LT-HSCs. In RNA-seq data, we found that KAI1 increases CDK inhibitors, which is mediated by PKC and TGFβ signaling pathways. Conversely, expression of CDK inhibitors was significantly reduced in LT-HSCs from *KAI1*$^{-/-}$ compared

to WT mice. Therefore, our data indicate that KAI1 is a master regulator of the cell cycle that maintains HSC dormancy and serves as a marker of LT-HSCs. To test whether the influence of KAI1 in LT-HSCs in mice could be extrapolated to humans, we examined human cord blood and found that KAI1 is also a marker of quiescent human LT-HSCs ($Lin^-CD38^-CD34^-CD93^+CD45RA^-$).

In this context, our study has major significance. First, KAI1 may be a crucial target molecule for *ex vivo* expansion of HSCs or for determining the regenerative capability of BM, which could be an important issue in clinical applications. Second, KAI1 may provide new insight in distinguishing normal HSCs from abnormal cells, such as leukemic stem cells that are able to escape antiproliferative chemotherapy. Further approaches will be needed to discover new molecules and mechanisms regulating quiescence and proliferation of HSCs.

FIGURE 1

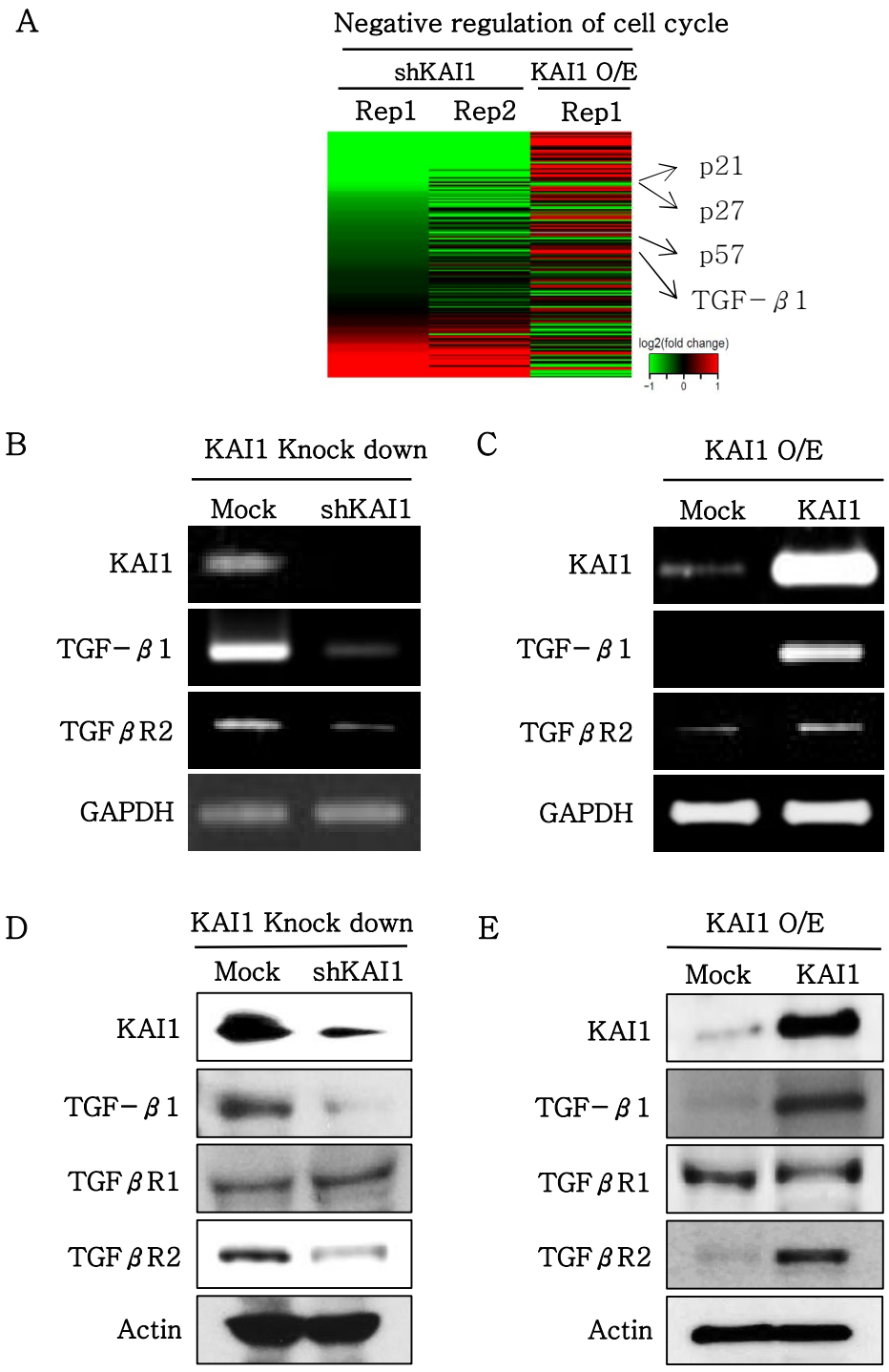
A
Negative regulation of cell cycle
shKAI1
KAI1 O/E
Rep1
Rep2
Rep1
p21
p27
p57
TGF−β1
log2(fold change)
−1
0
1
B
KAI1 Knock down
Mock
shKAI1
KAI1
TGF−β1
TGFβR2
GAPDH
C
KAI1 O/E
Mock
KAI1
KAI1
TGF−β1
TGFβR2
GAPDH
D
KAI1 Knock down
Mock
shKAI1
KAI1
TGF−β1
TGFβR1
TGFβR2
Actin
E
KAI1 O/E
Mock
KAI1
KAI1
TGF−β1
TGFβR1
TGFβR2
Actin

F

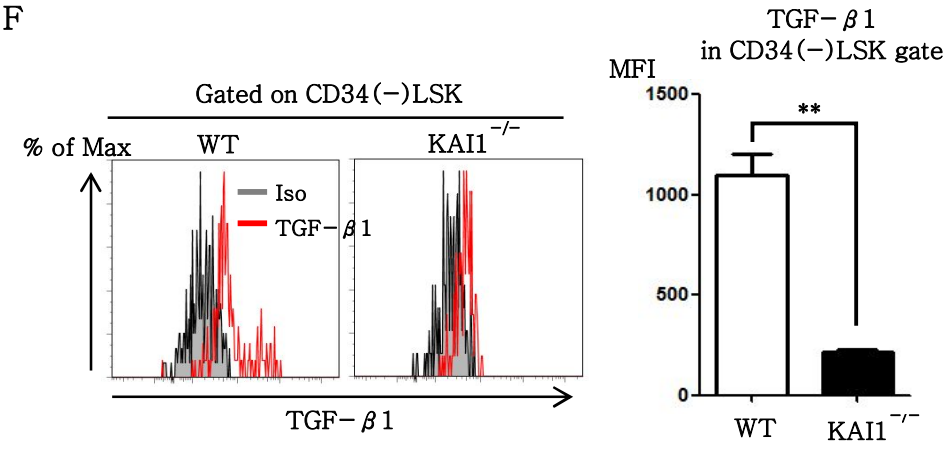
Gated on CD34(−)LSK
% of Max
WT
KAI1 −/−
Iso
TGF−β1
TGF−β1
TGF−β1
in CD34(−)LSK gate
MFI
1500
1000
500
0
**
WT
KAI1 −/−

G

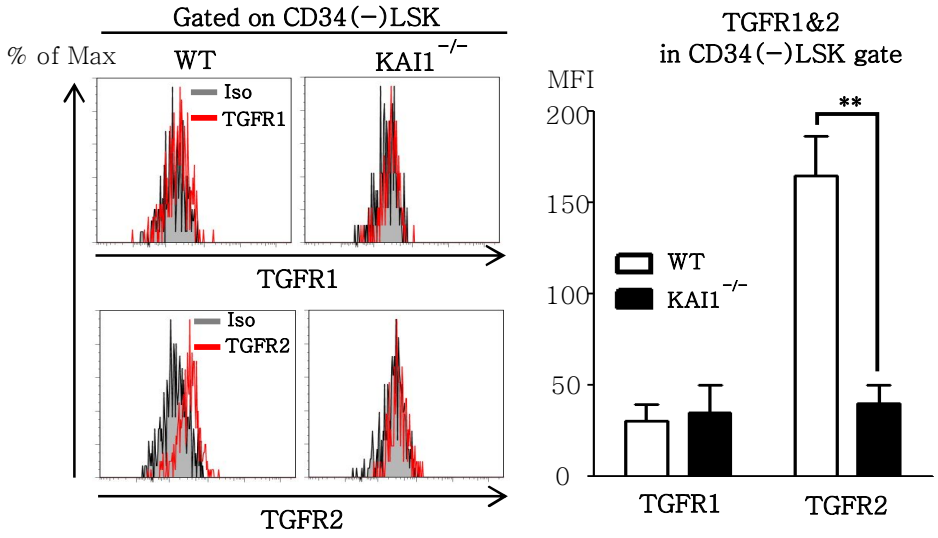
Gated on CD34(−)LSK
% of Max
WT
KAI1 −/−
Iso
TGFR1
TGFR1
Iso
TGFR2
TGFR2
TGFR1&2
in CD34(−)LSK gate
MFI
200
150
100
50
0
**
WT
KAI1 −/−
TGFR1
TGFR2

H

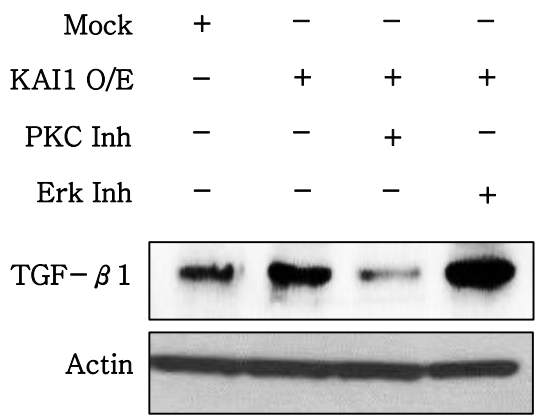
Mock + − − −
KAI1 O/E − + + +
PKC Inh − − + −
Erk Inh − − − +
TGF−β1
Actin

I

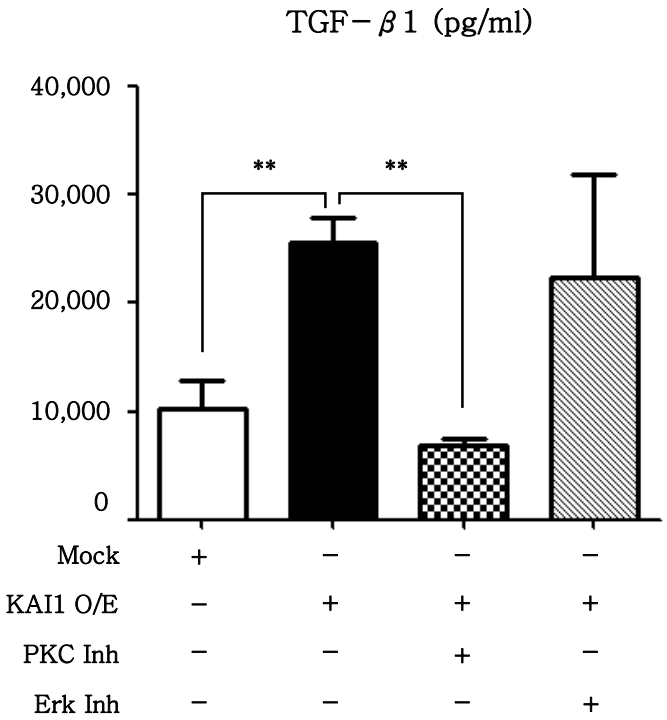
TGF−β1 (pg/ml)
40,000
30,000
20,000
10,000
0
**
**
Mock + − − −
KAI1 O/E − + + +
PKC Inh − − + −
Erk Inh − − − +

Figure 1. KAI1 activates TGF− β1and TGF βR2 via PKC

(A) RNA−sequencing data of EML cells after *KAI1* knock down or over−expression. (B, C) mRNA levels of TGF−β1 and TGFβR2 in EML cells after *KAI1* knock down and over expression. (D, E) Western blot analysis of KAI1, TGF−β1, TGFβR1 and TGFβR2 in EML cells after *KAI1* knock down and over−expression. (F, G) FACS analysis of TGF−β1, TGFβR1 and TGFβR2 expression in BM cells from WT and $KAI1^{-/-}$ mice (**p<0.05, n=3) (H, I) Western blot and ELISA analysis (n=3) of TGF−β1 in KAI1 over−expressed EML cells (**p<0.05).

FIGURE 2

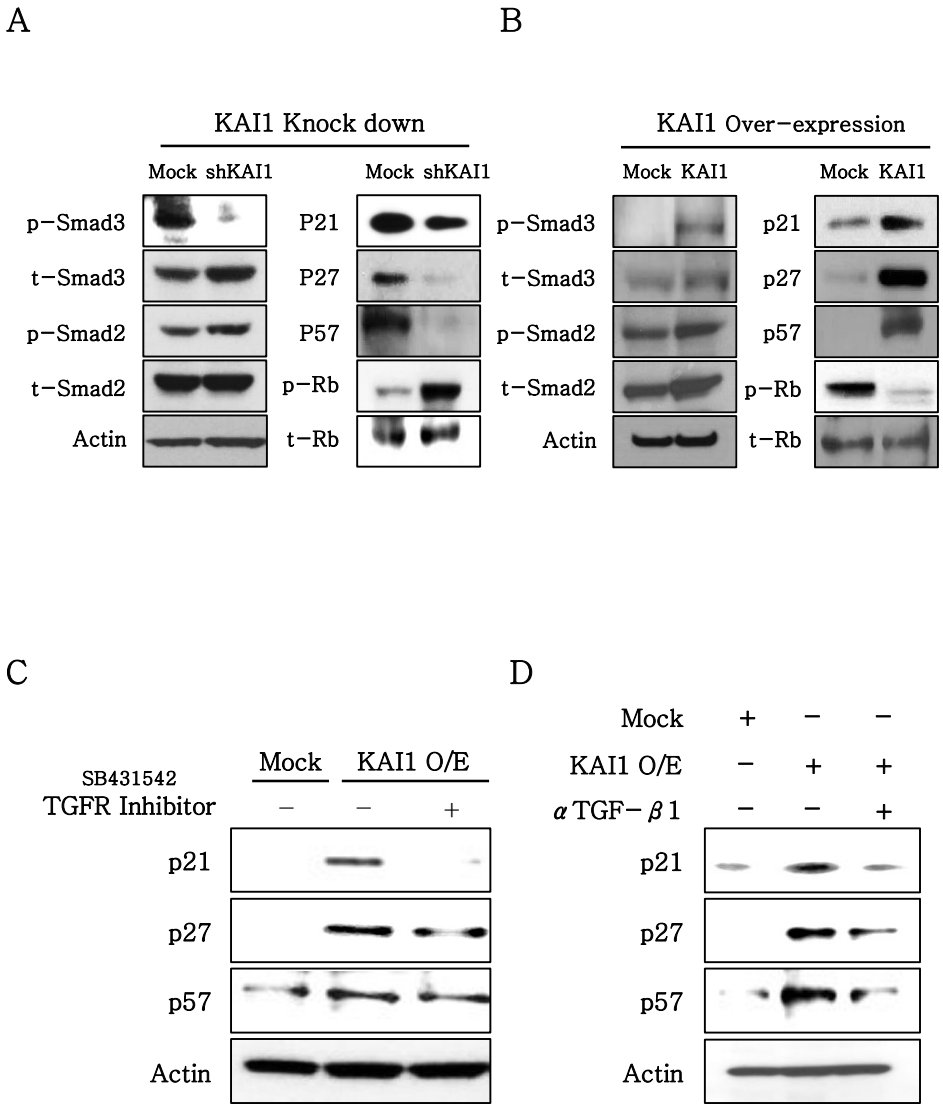
A
B
KAI1 Knock down
Mock shKAI1
Mock shKAI1
p-Smad3
t-Smad3
p-Smad2
t-Smad2
Actin
P21
P27
P57
p-Rb
t-Rb
KAI1 Over-expression
Mock KAI1
Mock KAI1
p-Smad3
t-Smad3
p-Smad2
t-Smad2
Actin
p21
p27
p57
p-Rb
t-Rb
C
D
SB431542
TGFR Inhibitor
Mock
KAI1 O/E
- - +
p21
p27
p57
Actin
Mock + - -
KAI1 O/E - + +
α TGF-β1 - - +
p21
p27
p57
Actin

E

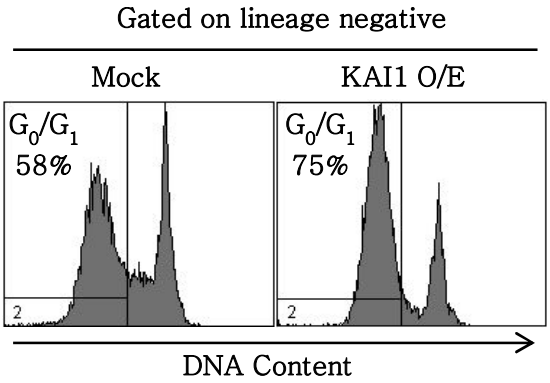
Gated on lineage negative
Mock
KAI1 O/E
G0/G1
58%
G0/G1
75%
2
2
DNA Content

F

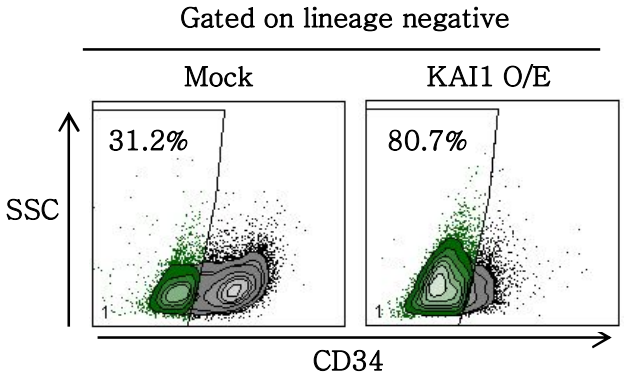
Gated on lineage negative
Mock
KAI1 O/E
31.2%
80.7%
SSC
1
1
CD34

Figure 2. KAI1 arrests the cell cycle of HSCs

(A, B) Phosphorylation levels of Smad2, Smad3, Rb and CDK inhibitors in EML cells after *KAI1* knock down or over-expression. (C) Induction of CDK inhibitors in EML cells after *KAI1* over-expression was blocked by the TGFβR inhibitor SB431542 (50 μM). (D) Induction of CDK inhibitors in EML cells after *KAI1* over-expression was blocked by a TGF-β1 neutralization antibody. (E) Cell cycle status of EML cells after mock and *KAI1* over-expression was determined by Hoechst 33342 staining. (F) EML cells were stained by lineage cocktail and CD34 antibodies after mock and *KAI1* over-expression.

FIGURE 3

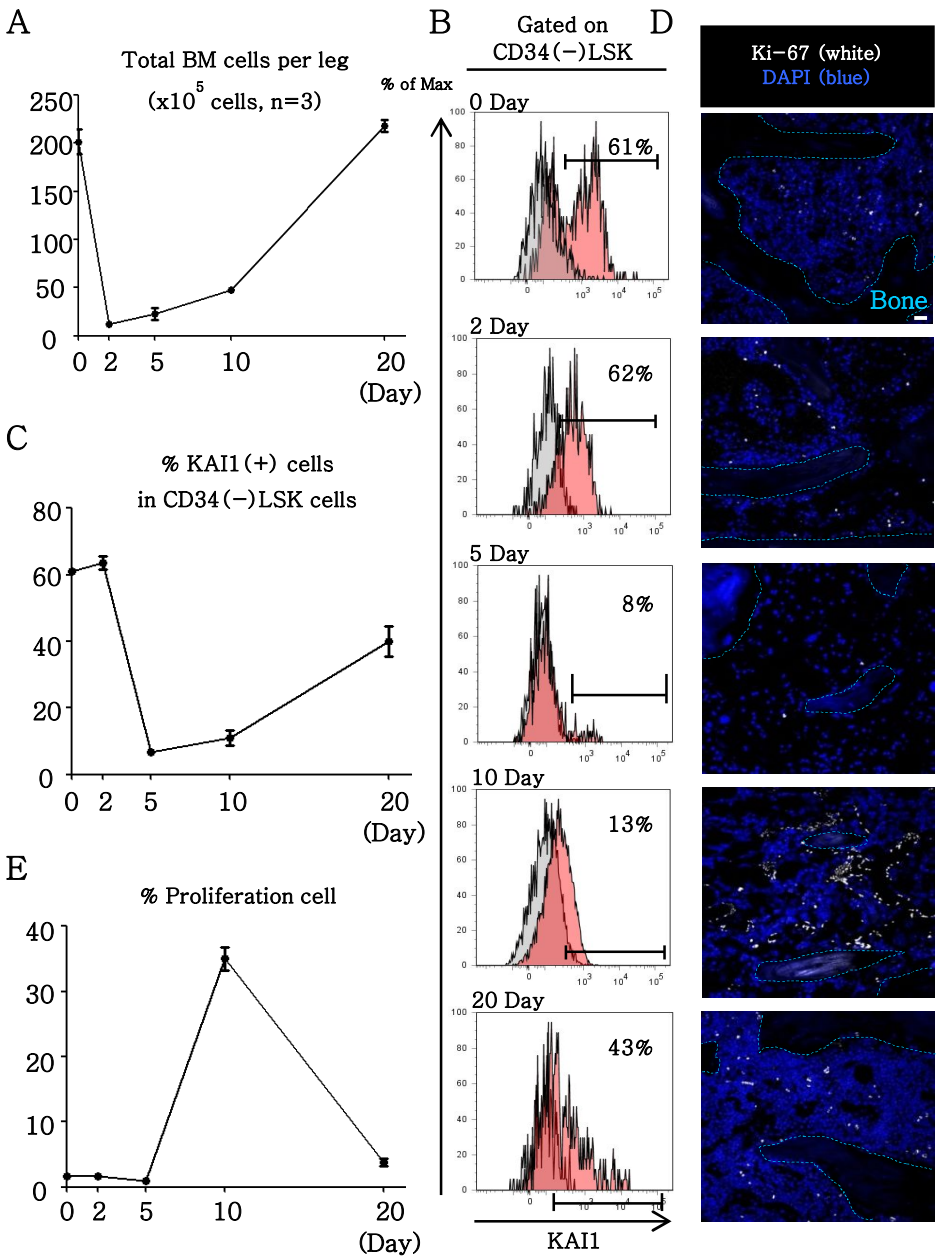
A
Total BM cells per leg
(x10^5 cells, n=3)
250
200
150
100
50
0
0 2 5 10 20
(Day)
B
Gated on
CD34(−)LSK
% of Max
0 Day
61%
2 Day
62%
5 Day
8%
10 Day
13%
20 Day
43%
KAI1
C
% KAI1(+) cells
in CD34(−)LSK cells
80
60
40
20
0
0 2 5 10 20
(Day)
D
Ki−67 (white)
DAPI (blue)
Bone
E
% Proliferation cell
40
30
20
10
0
0 2 5 10 20
(Day)

F

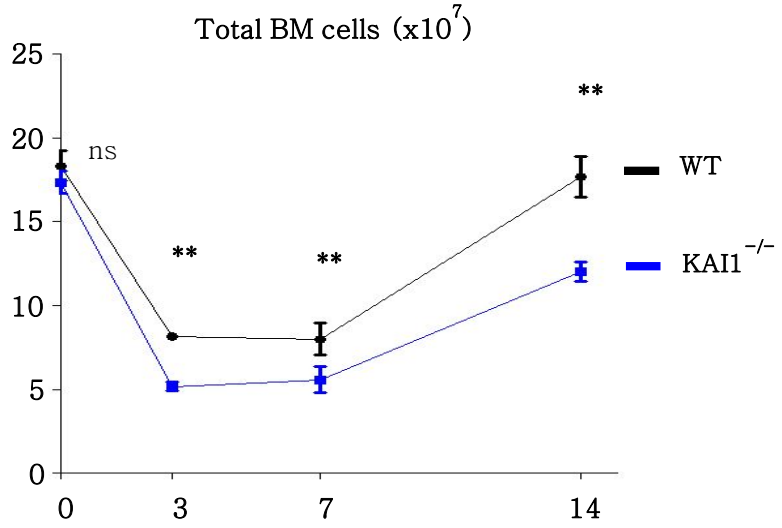
Total BM cells (x10^7)
25
20
15
10
5
0
ns
**
**
**
0
3
7
14
WT
KAI1 -/-

G

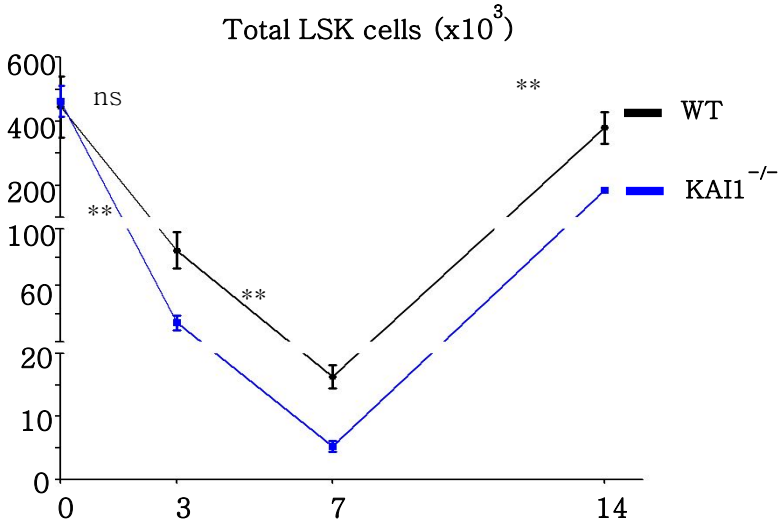
Total LSK cells (x10^3)
600
400
200
100
60
20
10
0
ns
**
**
**
0
3
7
14
WT
KAI1 -/-

Figure 3. Role of KAI1 in LT-HSCs to reconstitute the BM after ablation

(A) Total number of BM cells was counted at different time points after 5-FU injection (n=3). (B, C) Sequential change in $KAI1^{+}$ $LT^{-}HSCs$ in the BM after chemotherapy (n=3). (D, E) Representative figures of $Ki-67^{+}$ proliferating cells in the BM (n=3). Scale bar, 20 μm (F, G) WT and *KAI1*$^{-/-}$ mice were treated with sub-lethal irradiation and allowed to recover. Femurs and tibia were harvested at days 3, 7 and 14. Total numbers of BM (F) and LSK (G) cells were quantified, respectively (**$p<0.05$, n=3).

FIGURE 4

A

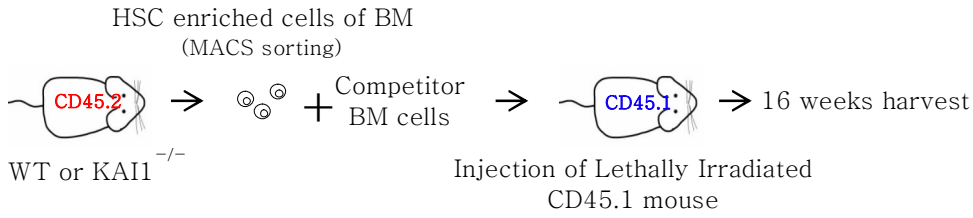

B

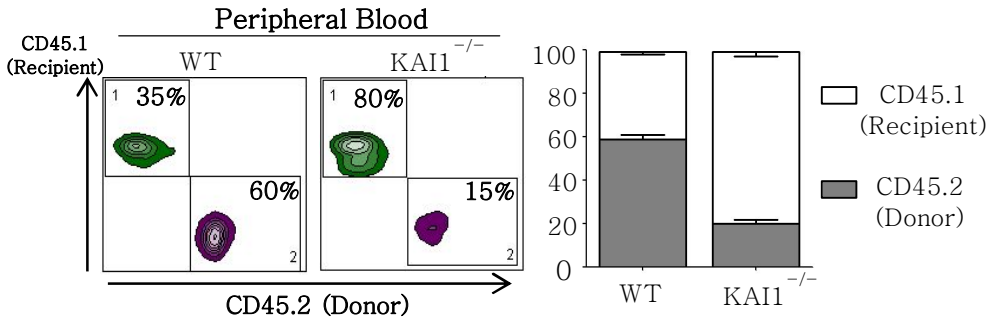

C

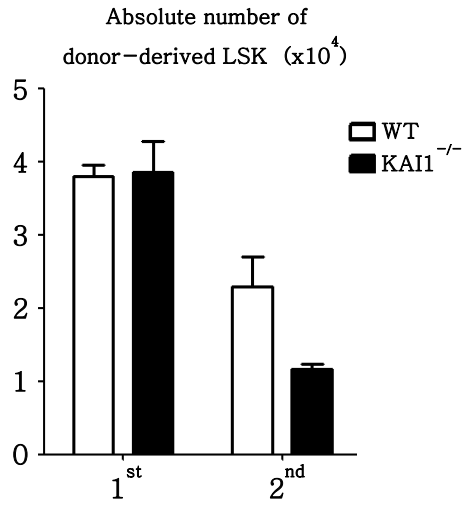

D

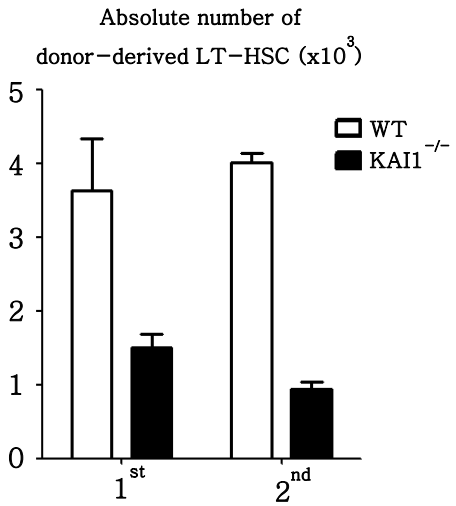

E

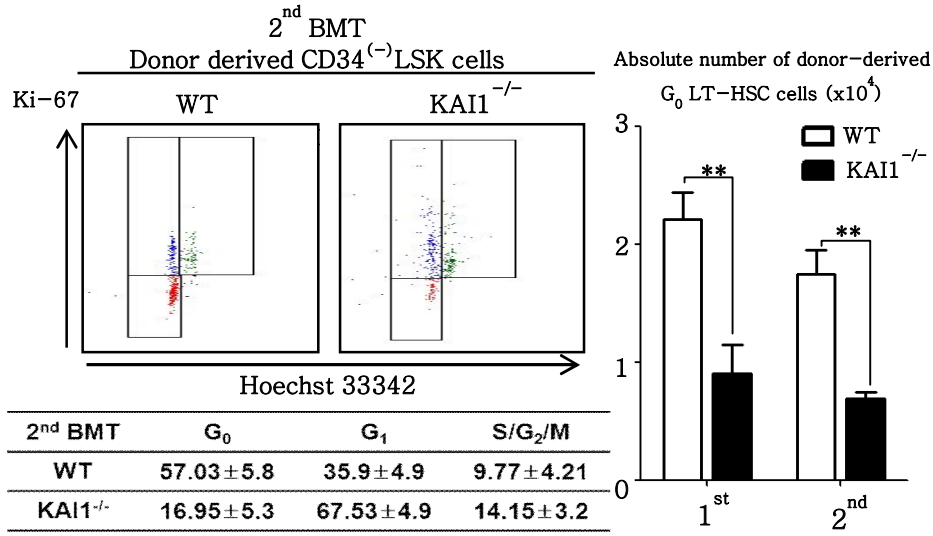

2nd BMT	G_0	G_1	$S/G_2/M$
WT	57.03±5.8	35.9±4.9	9.77±4.21
KAI1-/-	16.95±5.3	67.53±4.9	14.15±3.2

F

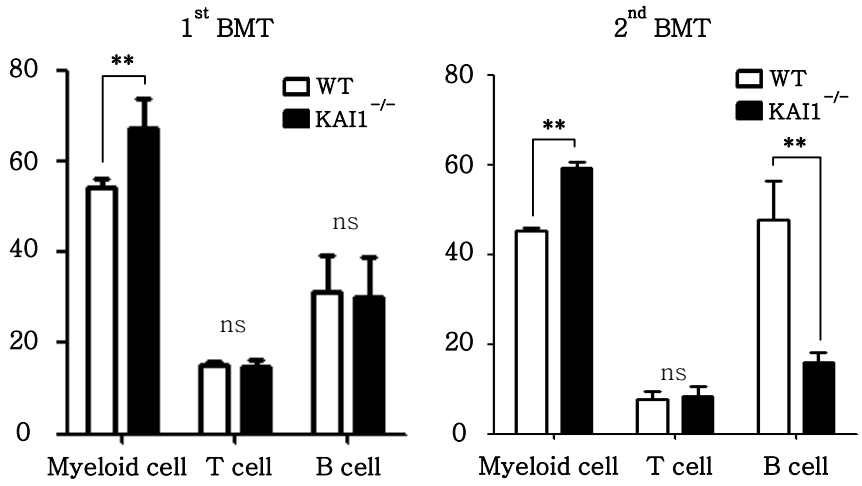

G

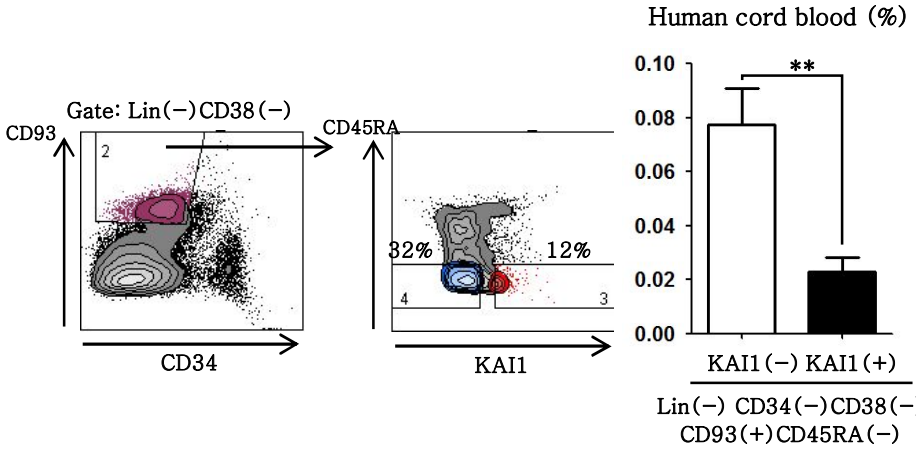
Human cord blood (%)
Gate: Lin(−)CD38(−)
CD93
CD34
CD45RA
KAI1
32%
12%
0.10
0.08
0.06
0.04
0.02
0.00
**
KAI1(−) KAI1(+)
Lin(−) CD34(−)CD38(−)
CD93(+)CD45RA(−)

H

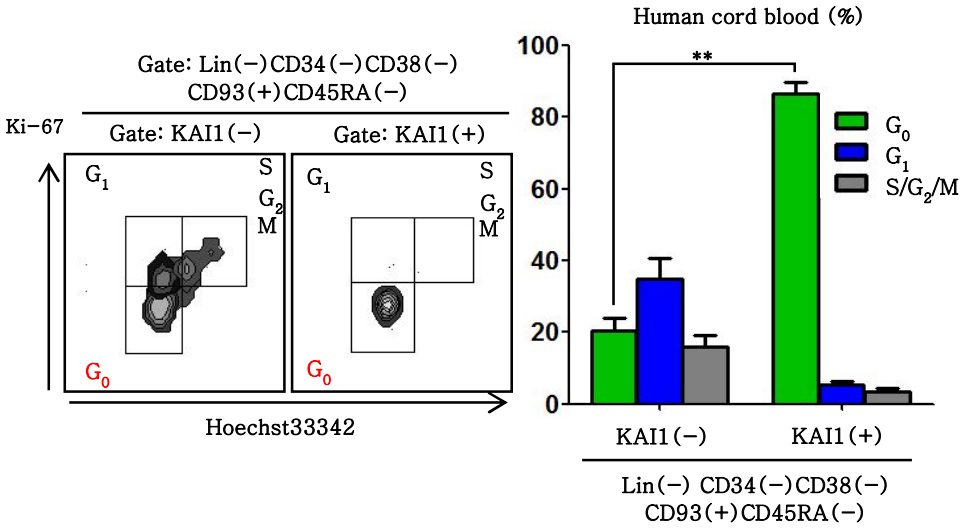
Human cord blood (%)
Gate: Lin(−)CD34(−)CD38(−)
CD93(+)CD45RA(−)
Ki−67
Gate: KAI1(−)
Gate: KAI1(+)
G1
S
G2
M
G0
Hoechst33342
100
80
60
40
20
0
**
G0
G1
S/G2/M
KAI1(−)
KAI1(+)
Lin(−) CD34(−)CD38(−)
CD93(+)CD45RA(−)

I

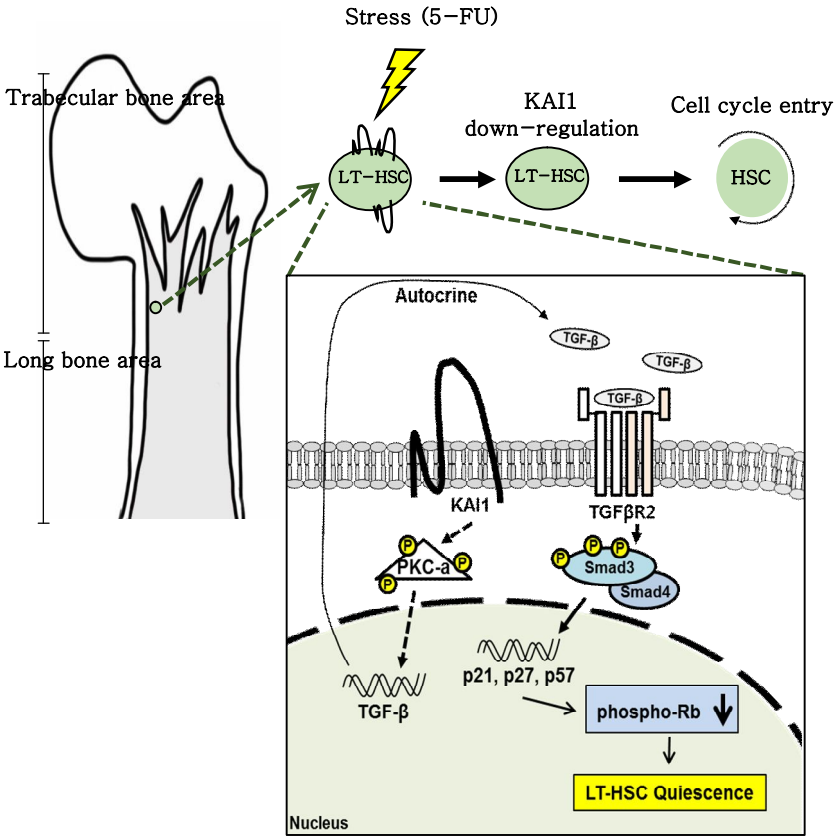
Stress (5-FU)
Trabecular bone area
Long bone area
LT-HSC
KAI1
down-regulation
LT-HSC
Cell cycle entry
HSC
Autocrine
TGF-β
TGF-β
TGF-β
KAI1
TGFβR2
PKC-a
Smad3
Smad4
p21, p27, p57
TGF-β
phospho-Rb
LT-HSC Quiescence
Nucleus

Figure 4. Role of KAI1 to repopulate blood cells after BMT and evidence of human KAI1+ LT-HSCs

(A) Schematic representation of the competitor transplantation. **(B)** Lethally irradiated recipient mice (CD45.1) were transplanted with Lin^- BM cells from WT and *KAI1*$^{-/-}$ mice (CD45.2) plus competitor cells (CD45.1). The bar graph shows the mean percentage of donor-derived (CD45.2) or recipient cells (CD45.1) in the peripheral blood 16 weeks after competitive BMT (**p<0.05, n=3). **(C, D)** The repopulating capacity of *KAI1*$^{-/-}$ and WT was determined through quantification of the absolute number of donor-derived LSK and LT-HSCs from recipient mice BM at week 16 after first and second transplantation. BM cells from recipient mice 4 months after first BMT were serially transplanted (**p<0.05, n=3). **(E)** Cell cycle analysis of donor-derived $CD34^-$ LSK cells from the BM of recipient mice at 16 weeks after first or second BMT. Quantification of the donor-derived G_0 LT-HSCs from the BM of recipient mice (**p<0.05, n=3). **(F)** The percentage of $CD11b^+$ myeloid cells, $CD3^+$ T cells, or $B220^+$ B cells from donor-derived cells from the BM of recipient mice

(**p<0.05, n=3). **(G)** FACS analysis of human umbilical cord blood derived LT-HSCs that were defined as $Lin^{-}CD38^{-}CD34^{-}CD93^{+}CD45RA^{-}$ cells (n=4). **(H)** Cell cycle analysis of $KAI1^{-}$ and $KAI1^{+}$ LT-HSC fractions derived from human umbilical cord blood (**p<0.05, n=3). **(I)** A scheme how KAI1 maintains LT-HSC quiescence in bone marrow.

References

Osawa, M., Hanada, K., Hamada, H., and Nakauchi, H. (1996). Long-term lymphohematopoietic reconstitution by a single CD34-low/negative hematopoietic stemcell. Science *273*, 242-245.

Rossi, D.J., Bryder, D., Zahn, J.M., Ahlenius, H., Sonu, R., Wagers, A.J., and Weissman,I.L. (2005). Cell intrinsic alterations underlie hematopoietic stem cell aging. Proceedings of the National Academy of Sciences of the United States of America *102*, 9194-9199.

Rossi, D.J., Jamieson, C.H., and Weissman, I.L. (2008). Stems cells and the pathways to aging and cancer. Cell *132*, 681-696.
Shen, Z.J., Esnault, S., Rosenthal, L.A., Szakaly, R.J., Sorkness, R.L., Westmark, P.R.,Sandor, M., and Malter, J.S. (2008).

Pin1 regulates TGF-beta1 production by activated human and murine eosinophils and contributes to allergic lung fibrosis. The Journal of clinical investigation *118*, 479-490.

Silberstein, L.E., and Lin, C.P. (2013). A new image of the hematopoietic stem cell vascular niche. Cell stem cell, 514-516.

Sims-Robinson, C., Zhao, S., Hur, J., and Feldman, E.L. (2012). Central nervous system endoplasmic reticulum stress in a murine model of type 2 diabetes. Diabetologia *55*, 2276-2284.

Stier, S., Ko, Y., Forkert, F., Lutz, C., Neuhaus, T., Grunewald, E., Cheng, T., Dombkowski, D., Calvi, L.M., Rittling, S.R.*, et al.* (2005). Osteopontin is a hematopoietic stem cell niche component that negatively regulates stem cell pool size. J Exp Med *201*, 1781-1791.

Sugiyama, T., Kohara, H., Noda, M., and Nagasawa, T. (2006). Maintenance of the hematopoietic stem cell pool by CXCL12-CXCR4 chemokine signaling in bone marro stromal cell niches. Immunity, 977-988.

Takubo, K., Goda, N., Yamada, W., Iriuchishima, H., Ikeda, E., Kubota, Y., Shima, H., Johnson, R.S., Hirao, A., Suematsu, M.*, et al.* (2010). Regulation of the HIF-1 alpha Level Is Essential for Hematopoietic Stem Cells. Cell Stem Cell, 391-402.

Tesio, M., and Trumpp, A. (2011). Breaking the cell cycle of HSCs by p57 and friends. Cell stem cell, 187–192.

Walkley, C.R., Shea, J.M., Sims, N.A., Purton, L.E., and Orkin, S.H. (2007). Rb regulates interactions between hematopoietic stem cells and their bone marrow microenvironment. Cell, 1081–1095.

Wei, Q., Huang, X.L., Lin, J.Y., Fei, Y.J., Liu, Z.X., and Zhang, X.A. (2011). Adeno associated viral vector–delivered and hypoxia response element–regulated CD151 expression in ischemic rat heart. Acta pharmacologica Sinica, 201–208.

Wu, J.Q., Seay, M., Schulz, V.P., Hariharan, M., Tuck, D., Lian, J., Du, J., Shi, M., Ye, Z., Gerstein, M.*, et al.* (2012). Tcf7 is an important regulator of the switch of self–renewal and differentiation in a multipotential hematopoietic cell line. PLoS genetics, e1002565.

Ye, Z.J., Kluger, Y., Lian, Z., and Weissman, S.M. (2005). Two types of precursor cells in a multipotential hematopoietic cell

line. Proceedings of the National Academy of Sciences of the United States of America, 18461-18466.

Yoshihara, H., Arai, F., Hosokawa, K., Hagiwara, T., Takubo, K., Nakamura, Y., Gomei, Y.,Iwasaki, H., Matsuoka, S., Miyamoto, K., *et al.* (2007). Thrombopoietin/MPL signaling regulates hematopoietic stem cell quiescence and interaction with the osteoblastic niche. Cell stem cell, 685-697.

Zon, L.I. (2008). Intrinsic and extrinsic control of haematopoietic stem-cell self-renewal. Nature *453*, 306-313.

Zou, P., Yoshihara, H., Hosokawa, K., Tai, I., Shinmyozu, K., Tsukahara, F., Maru, Y., Nakayama, K., Nakayama, K.I., and Suda, T. (2011). p57(Kip2) and p27(Kip1) cooperate to maintain hematopoietic stem cell quiescence through interactions with Hsc70. Cell stem cell

국문초록

조혈모작용은 골수 환경에서 휴지상태의 long term repopulating hematopoietic stem cells (LT-HSCs)에 의해 조절된다. KAI1은 tetraspanin superfamily에 속한 물질로 종양의 전이를 억제하는 유전자로 알려져 있었다. 본 연구는 KAI1이 골수에서 다른 stem-progenitor cells이 아닌 LT-HSCs에서만 발현하는 것을 확인하였다. KAI1 유전자 결핍 쥐를 제작하였으며 KAI1 유전자 결핍 쥐는 LT-HSC의 휴지상태를 잃게 되어 LT-HSC의 수가 선택적으로 감소하여 있음을 관찰 하였다. KAI1 유전자는 PKC를 통한 TGF-β1/Smad3 신호전달을 유도함으로써 세포주기를 조절한다. 또한 5-fluorouracil 처리에 의한 골수의 삭막 후에 골수세포에서 세포들의 회복이 KAI1 유전자 결핍 쥐에서 떨어짐을 확인 하였다. KAI1 유전자가 결핍 된 조혈모세포를 이식 받은 쥐는 정상적인 조혈모세포를 이식 받은 쥐들에 비해 LT-HSCs이 감소해 있음을 보였다. 또한 KAI1 유전자가 인간 LT-HSCs에서도 발현하고 있었으며 KAI1 유전자를 발현하고 있는 인간 LT-HSCs의 대다수가 휴지 상태 임을 확인 하였다. 이를 통해 KAI1 유전자는 이전에 밝혀지지 않은 LT-HSCs의 기능적인 표면 표지자 이며 LT-HSC의 휴지상태를 유지함을 보고 하는 바이다.

주요어 : LT-HSC, Quiescence, KAI1(CD82), Tetraspanin, Bone marrow, Stem cell niche

학번: 2013-22735